Optimized Heat Pump Design for GCC Countries, Part II: Baseline Chiller Instrumentation and Best Practice Guidance

M.T. Ali, H. Javed, M. Alhamahmy, P. R. Armstrong
Masdar Institute of Science and Technology

Abstract: Experimental data is necessary to train semi-empirical models for accurate modeling of physical operation of the chiller. Instrumentation of the chiller and steps taken to verify the accuracy of sensors used is described. Best practice recommendations are provided to minimize the errors during calibration and installation of sensors.

Key Words: Instrumentation Practices, Screw Chillers Performance

1 INTRODUCTION

Semi-empirical models rely on the accuracy of data used for their training. The data available in the publicly available datasheets of manufacturers is often limited in parameters and may not encompass the full range of weather and load conditions that the equipment undergoes during operation. Software available on different manufacturer's websites for simulating equipment performance provide no details of the models used for generating the data. Furthermore, use of simulated data for training models limits their ability to correctly predict the behavior of its different components.

However, acquisition of accurate real life data depends on the instrumentation and installation accuracy which can only be verified through the law of conservation of energy. The instrumentation inaccuracies depend on factors such as accuracy and repeatability of the sensor, installation details and quality, data logger capabilities such as accuracy and repeatability of voltage and frequency input measurements, electrical noise rejection capabilities, power supply precision and reference temperature sensor accuracy in case of thermocouples.

This paper presents the instrumentation details of 826kW air-cooled chiller and steps taken to verify the sensors accuracy individually and on the system level through heat balance checks.

2 CHILLER DESCRIPTION

An air-cooled chiller of 826kW capacity was selected to represent the typical cooling equipment used in Gulf Cooperation Council (GCC) countries to satisfy cooling load of commercial buildings. The chiller consists of two variable speed economized screw compressors in two separate refrigeration circuits. Each refrigeration circuit consists of a compressor, an oil separator, an air cooled condenser with six single-speed fans running in three pairs, a filter drier and a flash tank. The two refrigeration circuits feed a single shell and tube heat exchanger with two direct expansion evaporator circuits which provide cooling to the chilled water (CHW) circuit. The flash tank serves the dual purpose of providing additional cooling to the refrigerant going to

the expansion valve and provides intermediate cool vapor injection to the compressor.

The chiller is controlled by a built-in controller which selects the number of compressors to operate, compressor speeds, number of condenser fans to run, flash tank liquid level and degree of evaporator superheating. Two compressors are connected in parallel powered by a single variable speed drive (VSD). Cooling of the VSD in the chiller's electrical panel is provided by a propylene glycol circuit which rejects VSD heat to both of the two air-cooled condensers. The compressor motor is cooled by suction gas and (ISO VG120) Polyol Ester Oil (POE) which also serves to lubricate the compressor screws. The oil is separated from compressor discharge vapor using an oil separator and cooled in the air-cooled condenser connected with respective compressor as shown in Figure 1.

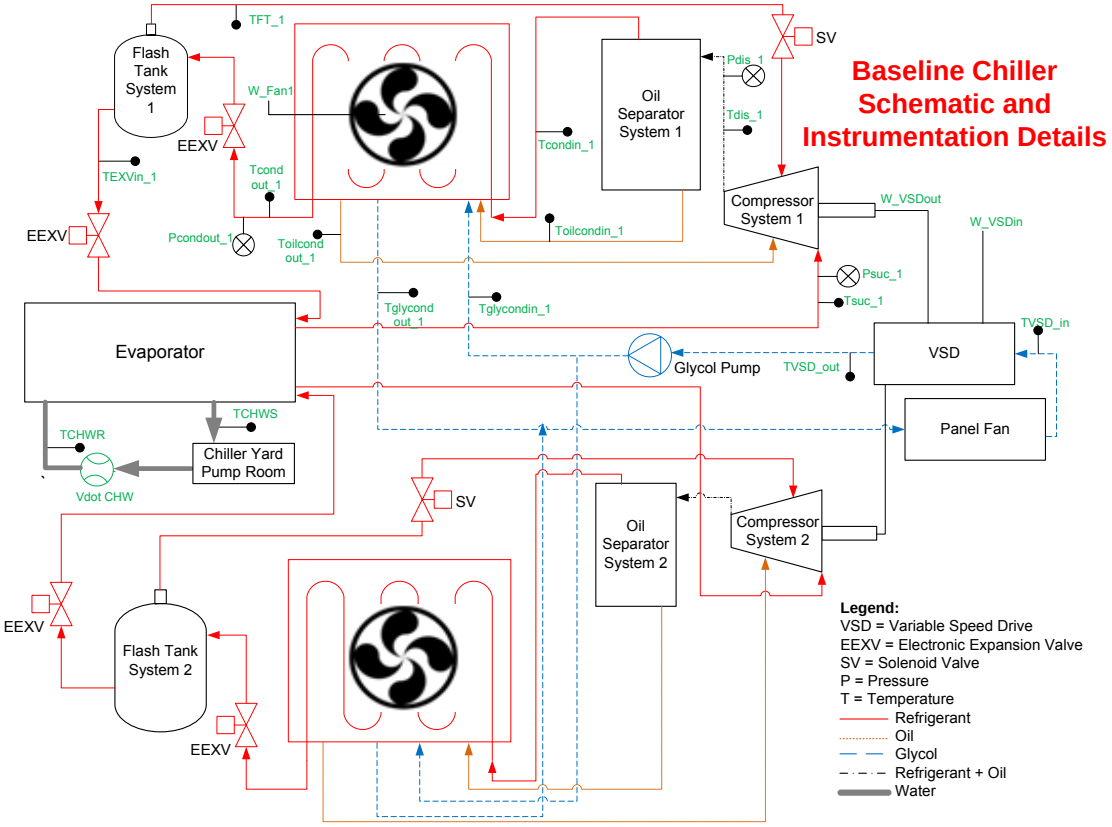

Figure 1: Baseline Chiller Schematic and Sensors Locations

3 INSTRUMENTATION DESCRIPTION:

System 1 of 413kW capacity is selected to characterize the performance of the chiller components. The built-in instrumentation necessary for safe and efficient operation of chiller does not provide the data at the inlet and outlet of each component and the parameters needed to compute the system energy balance. The system energy balance is needed to provide verification of instrumentation accuracy and calculation of refrigerant mass flow rate. Therefore additional sensors are needed to verify and train the individual chiller component models described in (H. Javed et al. 2014). The location and accuracy details of the instrumentation equipment are shown in Figure 1 and in Table 1.

Table 1: Instrumentation Technical Details

Equipment Type	Technical Specification	Function
Sealed Gauge Resistive Pressure Sensor	Accuracy: ±0.5%FS or ±0.1% BFLS	Measurement of discharge, condenser outlet and suction pressures
Special Limits of Error (SLE) Type T Thermocouple	Accuracy: ±0.5°C or ±0.4% of reading[1] (whichever is greater) (E230-ASTM)	Measurement of inlet and outlet temperatures of chiller components
Clamp-on Ultrasonic Flow Meter	Accuracy: ±0.5% of reading Repeatability: ±0.15% of reading	Measurement of chilled water flow rate
Current Sensor	Accuracy: ±1% of reading	Measurement of three phase currents of IGBT inlet and condenser fan and VSD output frequency
Power Meter	Accuracy: ±0.5% of reading	Measurement of IGBT inlet and condenser fan power
Analog Multiplexer with an isothermal metal bar	Reference temperature accuracy: ±0.4°C[2]	Measurement of thermocouples voltage
Data Logger with regulated 5V power supply and electrical noise rejection capability	Analog Inputs accuracy: ±0.18% of reading 5V Power Supply accuracy: ±4%[3]	Measurement, averaging and compilation of sensors data

[1] Realized accuracy is determined by logger's analog input accuracy which is ±0.18% of reading
[2] Measurements indicate better than ±0.1°C
[3] Measurements indicate better than ±0.5%

4 TEMPERATURE SENSORS INSTALLATION AND VERIFICATION:

4.1 Reference Temperature and Thermocouple Wire Verification:

The accuracy of energy balance across a chiller component depends on the accuracy of air-side and water-side differential temperature measurements. Therefore, the accuracy of absolute temperature measurement is not of primary concern. This was verified by putting three analog multiplexers from the same manufacturer in an insulated box shown in Figure 2. One of the three multiplexers channels were filled with SLE type T thermocouples. These thermocouples were put inside a copper pipe on one end to create an isothermal environment and 24cm of wire of each thermocouple was pressed next to the multiplexer's isothermal block to avoid stem error. The box was sealed airtight using silicone caulk and thermocouples were left inside the insulated box for 8 days.

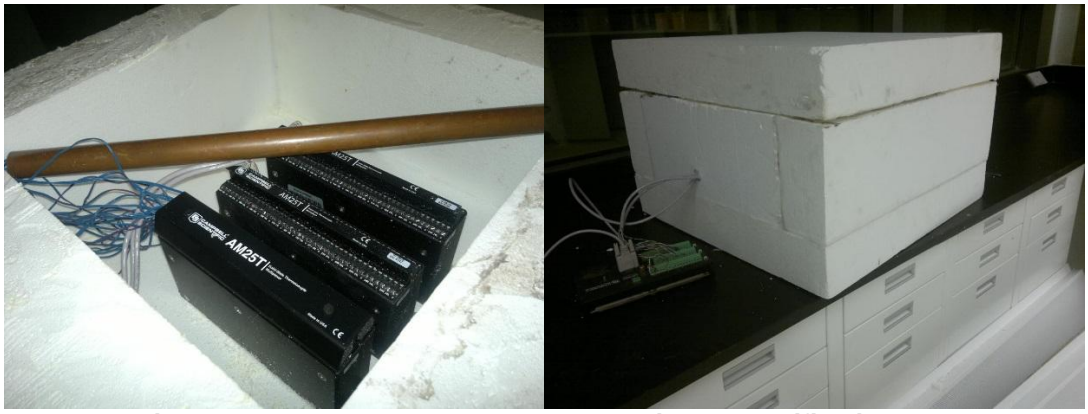

Figure 2: Temperature Measurement Equipment Verification Setup

The box was left for 3 days to equilibrate thermally with the environment. Averaged data of 360 readings taken at five second intervals were logged for the next 5 days. Figure 3(a) shows the residuals of reference temperature sensor of two multiplexers with reference to the multiplexer filled with thermocouples. It can be seen that the maximum difference between the three multiplexers was 0.05K. The difference between the twenty five thermocouples and their average is presented in Figure 3(b). It can be seen that the thermocouples agree with their average to within 10mK.

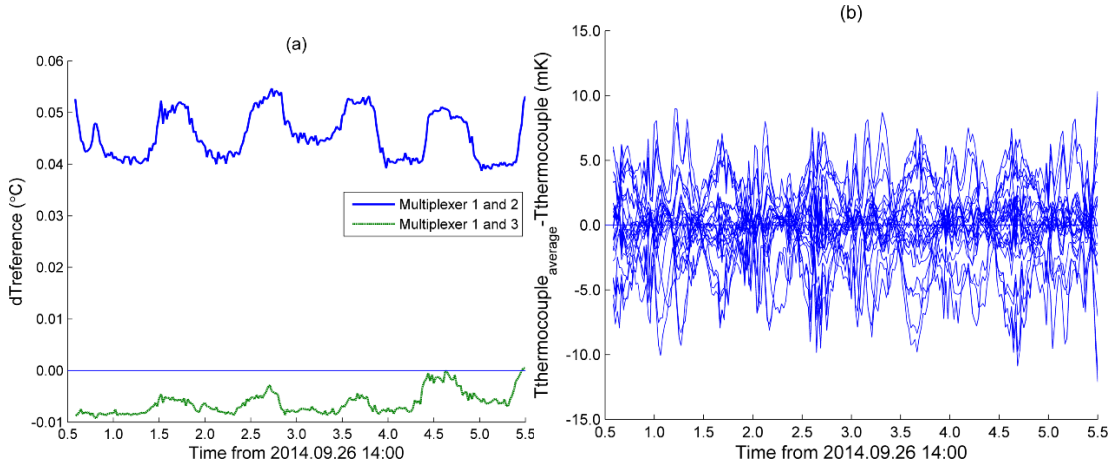

Figure 3: (a) Multiplexer Reference Temperature Comparison. (b) Thermocouples Difference with Their Mean

4.2 Refrigerant Temperatures Installation:

Type T thermocouples of #24 American Wire Gauge (AWG) were installed on the surface of the refrigerant copper piping at the locations shown in Figure 4. Surface temperatures are biased by conduction from fluid to ambient and by thermocouple stem error. Sensors were attached by epoxy to the copper pipe surfaces to bond an approximately 2cm thermocouple junction along with an approximately 6cm length of thermocouple lead wire at the sensor location. Two turns of thermocouple wire were made on the copper pipe at the sensor location and the whole assembly was wrapped by pre-tensioned silicon tape to ensure firm contact with the copper piping as shown in Figure 4. 10cm wide x 3cm thick closed cell foam rubber insulation was then wrapped on the sensor location to thermally insulate it from the surroundings.

Figure 4: Thermocouples Surface Installation

Stem error is mitigated by providing large area of contact and long lead wire length in the area of contact as thermocouples measure temperature by generating a potential difference at the junction which is conducted along the thermocouple wire (Richard M. Park 2010). Any large thermal gradient near the sensor location and at the termination point can affect thermocouple measurement accuracy.

4.3 Chilled Water Temperature Difference Verification:

Thermocouples were installed initially on chilled water pipe surfaces as was done for refrigerant side copper piping. The pipes are nominal 250mm schedule 40 pipe made of carbon steel. This led to a very poor system energy balance. Two thermocouples were then glued on the tip of the 10mm diameter RTDs in the thermowells used by the chiller built-in water temperature sensors for controlling compressor speed. The thermowells were filled with oil to eliminate air. Later on, 1.5mm sheathed thermocouple probes were inserted in the chilled water supply and return lines and lastly a probe of equal area spaced five thermocouples were installed on the chilled water supply line to measure the temperature gradient on the evaporator outlet of the chilled water side (Armstrong, P.R. et al. 1993). Another 1.5mm probe on Chilled Water Supply (CHWS) was inserted 3.5m downstream of the CHWS line for comparison.

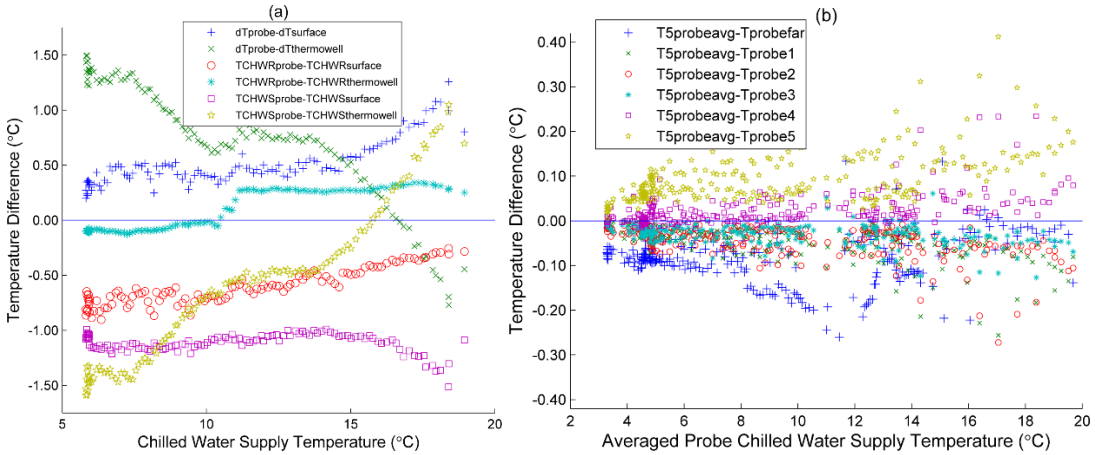

Figure 5: Chilled Water Temperature Sensors Comparison

Figure 5(a) show the difference between the differential temperatures measured by the three different sensor installations and also the difference between the return and supply sensor installations. It can be seen that the surface differential measurement had an error of 0.5K for majority of the points. The difference at the Chilled Water Return (CHWR) side between the probe and surface is 0.6K which increases to 1.1K on average indicating that the surface measurement on carbon steel pipes should be avoided. The thermowell installations on the chilled water side suffered from water condensation indicating lack of proper seal of cable glands through which the RTD wire comes out of the thermowell. This is prominent at the CHWS location. The plateau occurring at CHWS temperature of 14.01°C is due to condensation as during this period the air dew point temperature varied from 14-15°C as determined from a weather station located about 1km NW of the chiller yard.

Figure 5(b) presents the difference between the average of the five thermocouple probe measurement with the individual probes and the probe inserted 3.5m downstream in the CHWS line. It can be seen that the probes located near the middle of the pipe agree with the average to within 0.02K for majority of the data points. The difference increases to 0.04K for the probe located near the bottom of the pipe while the difference at the top of the pipe is greater than 0.1K for majority of the data points. This increase in error for the probe located near the top can be attributed to presence of air bubbles in the water or thermal stratification.

The probe inserted 3.5m downstream of the CHWS line is located after an elbow. Figure 5(b) shows that the probe is within 0.01K when the CHWS temperature is closer to ambient. This shows that locating a single probe in a well-mixed fluid flow is sufficient. However, this error increases to 0.1K on average when the difference between CHWS temperature and ambient increases which can be attributed to jacket loss.

4.4 Condenser Air Side Temperature Difference Verification:

Temperature differences across the air cooled condenser were measured using three thermopiles. Thermopiles placed across fan 1, 4, 5 and 6 consisted of eight thermocouple junction pairs while thermopile placed across Fan 3 and Fan 4 consisted of twelve thermocouple junction pairs. Each thermopile covered a condenser face area of 5.42m^2. The fan numbering starts from the fan present at the inlet of the condenser shown in the bottom of Figure 6. The thermopiles were placed across the six condenser fans which are operated as three pairs as follows: Initially fans 1 and 6 are turned on, then fans 2 and 3 and lastly fans 4 and fan 5 come into operation. The pairs separated by baffles to minimize cross-flow of air. The voltage generated by the thermopiles was converted to temperature difference using the procedure described in (Armstrong, P.R. 1983). A verification of the thermopile temperature measurements was made by placing a high density rake of twenty five thermocouples spaced according to equal area method on the condenser fan discharge as shown in Figure 6. An experiment was conducted by placing the rake on each fan and logging the temperature measured by the thermocouple rake. The temperature difference was then computed taking the difference of inlet air temperature measured by a thermocouple located in the middle of the condenser beneath the condenser frame.

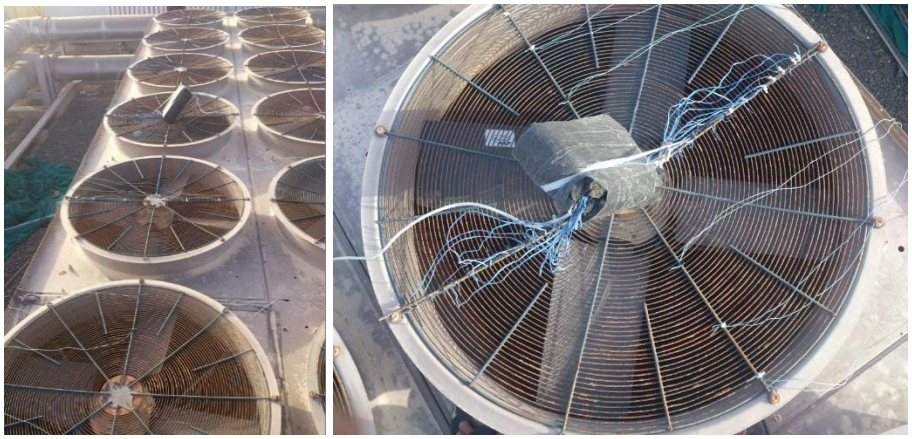

Figure 6: Condenser Fan Thermopile and Thermocouple Rake Installation

Table 2 shows the difference between the thermopile and condenser rake average of fan pairs on which the thermopiles are installed. It can be seen that an eight junction thermopile is not sufficient to accurately measure temperature difference while a twelve junction thermopile had an error of 2%. However, the overall difference across the condenser between the rake and the thermopile differential measurement remained within 0.6%.

Table 2: Thermopile Temperature Measurement Verification

	Fan 1	**Fan 2**	**Fan 3**	**Fan 4**	**Fan 5**	**Fan 6**
$\frac{(dT_{rake}-dT_{thermopile})}{dTrake}$ (%)	14.97	0.08	-3.88	-4.89	-2.76	-0.18
	Fan 1 and Fan 6 Average (8 pair)		Fan 2 and Fan 3 Average (12 pair)		Fan 4 and Fan 5 Average (8 pair)	
$\frac{(dT_{rake}-dT_{thermopile})}{dTrake}$ (%)	7.39		-2.00		-3.82	

5 PRESSURE SENSORS VERIFICATION:

Pressure sensors of 300psi were installed to measure the pressure across the compressor as well as to determine refrigerant state at key points in the chiller's thermodynamic cycle. The stated accuracy was verified using a dead weight tester prior to their installation using the procedure mentioned in Precision Pressure Measurement: User Guide to Pressure Measurement (2013). A least squares line was fit on the experimental data instead of the end-point line used for 0.5-4.5V analog output pressure sensors. It can be observed from Figure 7(a) that the maximum measurement error in the readings of the transducers was around 0.6% or more. After calibration these errors are within ±0.16% of span.

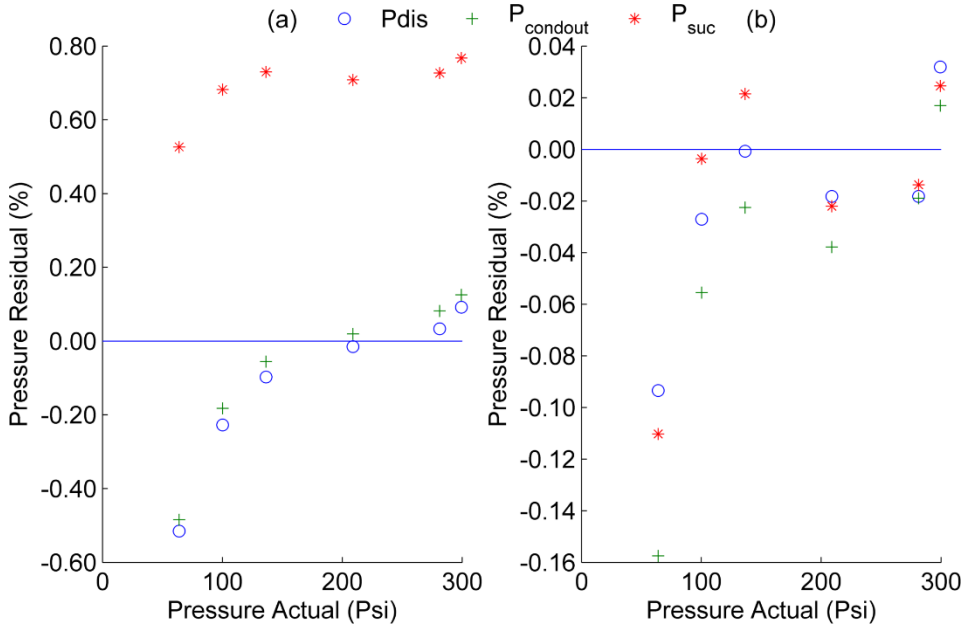

Figure 7: (a) Pressure Residuals before Calibration (b) Pressure Residuals after Calibration

6 AIR FLOW RATE VERIFICATION:

Air flow rates of condenser fans were measured using a thermal anemometer of an accuracy of ±[0.03m/s+5% of reading]. The thermal anemometer was calibrated in a Particle Image Velocimetry (PIV)-calibrated bench-top wind tunnel. A least squares line was fitted to the data. It can be observed from Figure 8(a) that the maximum measurement error in the readings of the anemometer was 5.6%. After calibration these errors are ±4%.

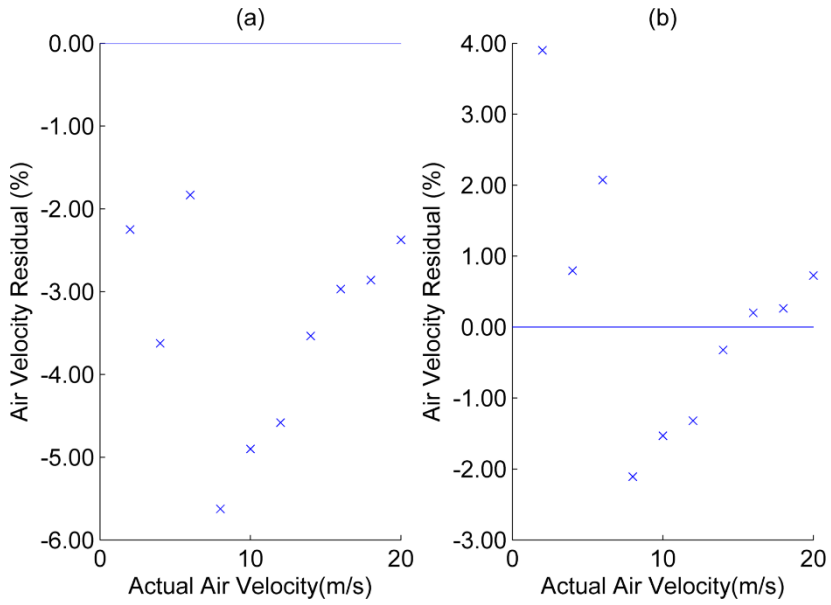

Figure 8: (a) Air Velocity Residuals before Calibration (b) Air Velocity Residuals after Calibration

There are two condenser inlet faces, front and back, for each fan. The average face velocity over each inlet surface was estimated by measuring the velocities at each of sixteen points of measurement shown in Figure 9(b), with four trials for each measurement (Benedict 1984). The thermal anemometer was found to be very sensitive to wind. Therefore, a screen was erected around the condenser to minimize the effect of wind as shown in Figure 9(a).

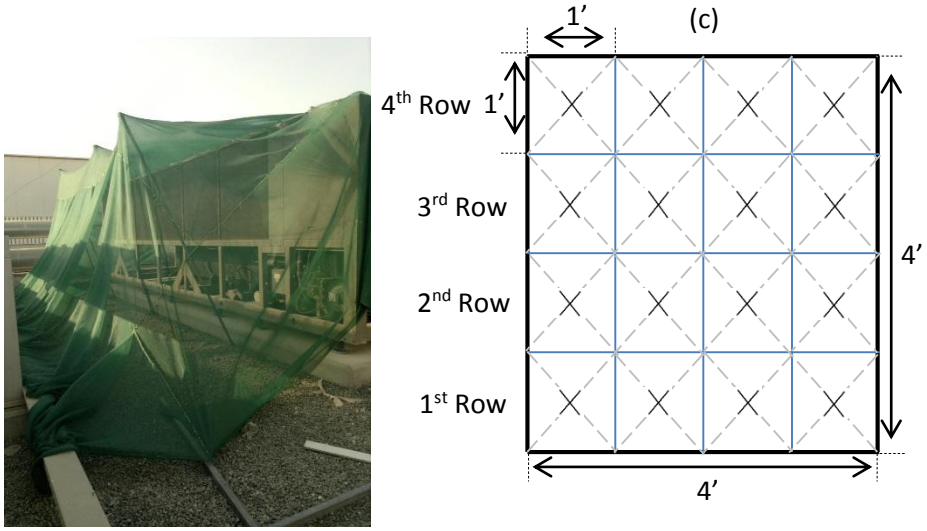

Figure 9: (a) Screen for Minimizing Wind Effect (b) Locations of Traverse Airflow Measurements on Each Air-Side Inlet Face Indicated by "X"

Table 3 presents the velocities measured at the locations shown in Figure 9(b) for Fan 1. It can be seen that air velocity on the back side of the condenser inlet remains uniform with a standard deviation of 0.15m/s with the top three rows having a standard deviation of only 0.03m/s. These rows on the back side are shielded from the wind effects. However, the air velocity readings on the front have a standard deviation of 0.22m/s with the top two rows near the edge of the screen indicating 16% higher velocity as compared to the back side. Therefore, back side average of the air velocity was taken which resulted in a flow rate of 6.48 m^3/s. This flow rate was multiplied by the numbers of fans operating to compute the condenser air flow rate. This flow rate was found to be 8% higher than the chiller technical data sheet.

Table 3: Average of Four Measurements of Air Velocity on Condenser Inlet

Row	Back Side Air Velocity (m/s)				Average (m/s)	Front Side Air Velocity (m/s)				Average (m/s)	Difference[1] (%)
4th	2.59	2.29	2.33	2.43	2.41	2.66	2.90	2.89	2.81	2.81	16.7
3rd	2.36	2.46	2.40	2.31	2.38	2.80	2.82	2.82	2.76	2.80	17.5
2nd	2.15	2.40	2.42	2.42	2.35	2.49	2.55	2.55	2.45	2.51	7.0
1st	2.09	2.10	2.05	2.07	2.08	2.30	2.44	2.38	2.36	2.37	14.1
			Average (m/s)		2.30			Average (m/s)		2.62	

[1] Percentage difference between front and back

7 ELECTRICAL POWER VERIFICATION:

Power is the product of instantaneous (not rms) current and voltage. The transducers installed for measuring current were calibrated to 0.1%FS using a reference current source and a reference current transducer with an accuracy of ±0.02% for 120:1 ratio of input current (Arbiter Instruments 2008). The power inputs to the compressor's variable speed drive and condenser fans were measured by pulse output power transducers with 333mVrms current transducer inputs. The response of each power and current transducer set was verified by one-time simultaneous measurement using a portable power analyzer of ±1% accuracy (Fluke Corporation 2013). The active power measured by the two methods agreed within better than 1% of each other.

8 ENERGY BALANCE VERIFICATION:

The energy balance equation used for verification of instrumentation is given by Equation 1:

$$\dot{m}_{air} * Cp_{air} * \dot{dT}_{air_{cond}} = W_{compin} + \dot{m}_{CHW} * \left(h_{CHW_{in}} - h_{CHW_{out}} \right) \quad (1)$$

The component energy balance check was carried out for the condenser using the energy conservation equations for each chiller component which are given by Equations 2-7. The VSD efficiency 'η_{VSD}' is taken as 98% which was obtained from one-time measurement of VSD output power at maximum compressor speed.

Compressor:

$$\dot{W}_{compin} * \eta_{VSD} = \dot{m}_{ref-oil} * h_{dis} - \dot{m}_{ref_{evap}} * h_{suc} - \dot{m}_{ref_{flash-gas}} * h_{flash-gas} - \dot{m}_{oil} * h_{cond_{out}} \quad (2)$$

Oil separator:

$$\dot{m}_{ref-oil} = \dot{m}_{ref} + \dot{m}_{oil} \quad (3)$$

$$\dot{m}_{ref} = \dot{m}_{ref_{evap}} + \dot{m}_{ref_{flash-gas}} \quad (4)$$

Flash Tank:

$$\dot{m}_{ref} * h_{cond_{out}} = \dot{m}_{ref_{flash-gas}} * h_{flash-gas} + \dot{m}_{ref_{evap}} * h_{evap} \quad (5)$$

Evaporator:

$$\dot{m}_{ref_{evap}} * \left(h_{suc} - h_{evap_{in}} \right) = \dot{m}_{CHW} * \left(h_{CHW_{in}} - h_{CHW_{out}} \right) \quad (6)$$

Condenser:

$$\dot{m}_{air} * Cp_{air} * \dot{dT}_{air_{cond}} = \dot{m}_{ref} * \left(h_{cond_{in}} - h_{cond_{out}} \right) + \dot{m}_{oil} * \left(h_{oilcond_{in}} - h_{oilcond_{out}} \right) \quad (7)$$

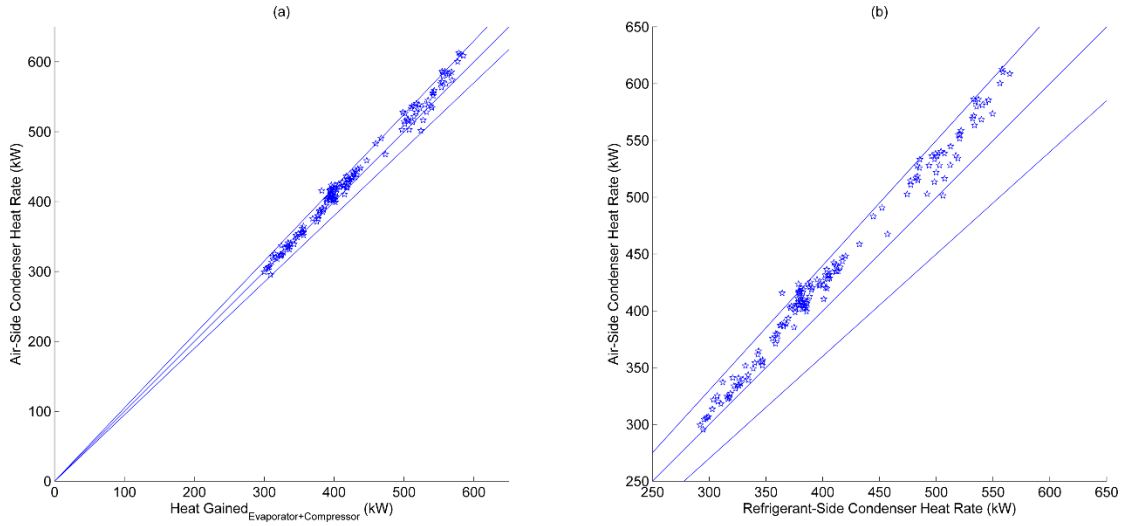

Figure 10: (a) System Energy Balance Check (b) Condenser Energy Balance Check. Lines at ±10% are shown in (a) and at ±5% in (b)

Equations 2-6 are solved simultaneously to obtain refrigerant and oil flow rates. Equation 7 is then used to check for energy conservation accuracy. It can be seen from Figure 10(a) and (b) that the energy balance was achieved to within 5% for the system and within 10% for the condenser. The glycol loop heat input is excluded from the energy balance which results in a lower heat rate computed on the condenser refrigerant-side.

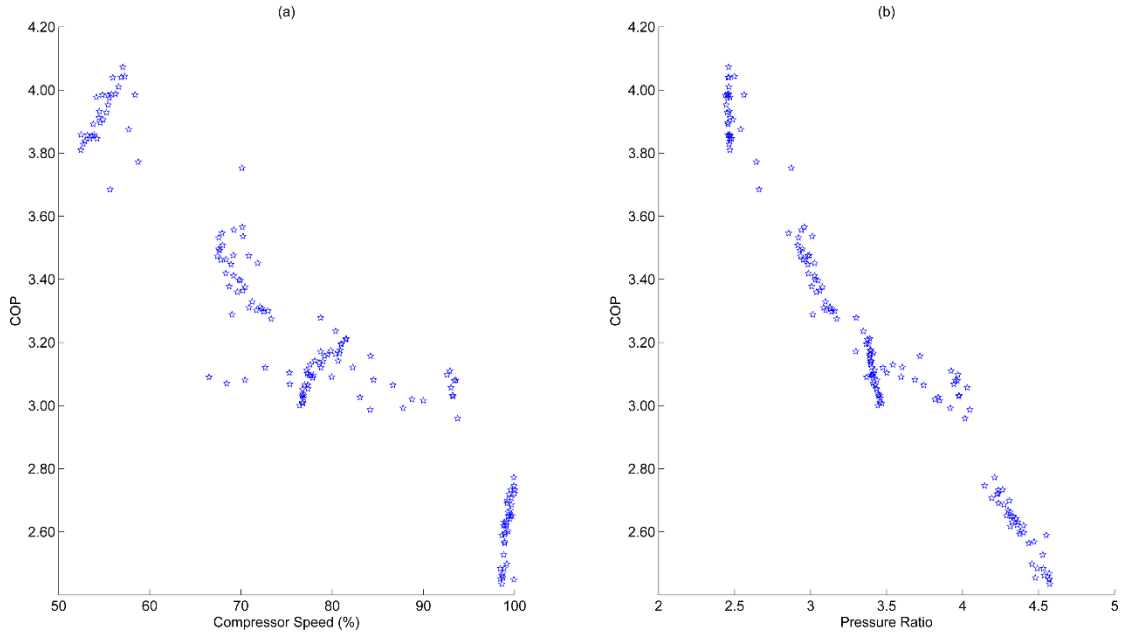

Figure 11: (a) System COP vs Compressor Speed (%) (b) System COP vs Pressure Ratio

Figure 11(a) and (b) present the system COP for a range of compressor speed and pressure ratio of the baseline chiller. The increase in system COP with decreased pressure ratio as shown Figure 11(b) follows a more distinct profile than as a function of speed because COP is a stronger function of pressure ratio.

9 CONCLUSION:

Acquisition of reliable data depends on the accuracy of the sensors, data sensing equipment and sensors installation. The instrumentation accuracy can be verified by system energy balance. An accurate system energy balance is necessary to estimate refrigerant and oil flow rates during operation necessary for training semi-empirical models of chiller components. The instrumentation of the baseline chiller provided valuable experience on the behavior of parameters that can affect energy balance.

It is concluded from the data acquired during CHW side temperature measurements that surface temperature measurement on steel pipes should be avoided. Furthermore, thermowells should be isolated from environment using water tight cable glands and filled with thermal grease to avoid water penetration. A fluid mixing device installed before the temperature measurement location may be used to minimize measurement error due to thermal stratification on the CHWS side. Furthermore, a higher number of thermopile junction pairs is recommended for high thermal gradient air side areas. However, further experimentation is needed to come up with a recommendation for ratio of condenser face area to thermopile junction pairs.

Surface temperature measurements on copper piping are adequate if good thermal contact is ensured and steps are taken to avoid stem error for thermocouples. A least squares line increases the accuracy of ratiometric pressure sensors significantly instead of using an end-point line. Lastly, efforts should be taken to minimize wind disturbance (air turbulence) before performing condenser air flow rate measurements by thermal anemometers.

10 ACKNOWLEDGEMENT :

We thank Executive Affairs Authority (EAA) and Masdar Institute of Science and Technology for supporting this research. In addition, thanks to Hanif Shaikh, Alex Niswander, Omer Sarfraz, Jemal Adam and Akmaljon Khusanov for help with installation of instrumentation.

11 REFERENCES:

Arbiter Instruments. (2008). “Technical Datasheet”. Arbiter Instruments.

Armstrong, P.R. (1983). “Instrumentation of Solar Heating and Cooling Systems at CSU.” In *Second Annual Workshop on Performance Monitoring*. Florida Solar Energy Center,.

Armstrong, P.R., C.R. Batishko, A.L. Dittmer, D.L. Hadley, and J.L. Stoops. (1993). “Mobile Energy Laboratory Procedures”. PNNL-8838.

Benedict, R.P. (1984). “Temperature, Pressure, and Air Flow Measurement”. 3rd ed. John Wiley & Sons, Inc.

“E230- Standard Specification and Temperature-Electromotive Force (EMF) Tables for Standardized Thermocouples.” (2003). ASTM International.

Fluke Corporation. (2013). “Technical Datasheet”. Fluke Corporation.

H. Javed, O. A. Qureshi, M.T.Ali, and P. R. Armstrong. 2014. “Optimized Heat Pump Design for GCC Countries, Part I: Algorithm.” In *Proceedings of the 11th International Energy Agency Heat Pump Conference*.

“Precision Pressure Measurement: User Guide to Pressure Measurement”. (2013). AMETEK.

Richard M. Park. (2010) “Thermocouple Fundamentals”. Cleveland, Ohio, U.S.A.: Marlin Manufacturing Corporation.